

14% EFFICIENT LARGE AREA SCREEN PRINTED STRING RIBBON SOLAR CELLS

Giso Hahn¹, Alexander Hauser¹, Andrew M. Gabor²

¹Universität Konstanz, Fachbereich Physik, Fach X916, 78457 Konstanz, Germany

Tel.: +49-7531-88-3644, Fax: +49-7531-88-3895

E-mail: giso.hahn@uni-konstanz.de

²Evergreen Solar, Inc., 259 Cedar Hill St., Marlboro, MA 01752-3004, USA

ABSTRACT: String Ribbon silicon by Evergreen Solar just made the step from pilot line to large scale production. A new plant has been opened recently in Marlboro (MA, USA) and production is currently ramping up. In this stage it is helpful to determine the potential in efficiency of the current material used for production. In this way single processing steps can be checked and adjusted. Therefore partly processed wafers in different stages of processing have been shipped from Evergreen Solar to University of Konstanz (UKN) and vice versa. Additionally, two reference batches have been processed completely at Evergreen and UKN respectively. A gap of 1.7% absolute in efficiency could be detected between the Evergreen and UKN processes. By exchanging the single processing steps the influence of each step (diffusion, SiN, metallisation) on efficiency could be detected, with the diffusion showing the largest influence. The best cell of the UKN process showed an efficiency of 14.3% ($8 \times 10 \text{ cm}^2$) using a $40 \text{ } \Omega/\text{sq}$ emitter. This is the highest efficiency obtained so far on a large area String Ribbon solar cell. Higher sheet resistivities should lead to efficiencies $>14.5\%$ in the near future. The best large area String Ribbon cell processed at Evergreen to date showed an efficiency of 13.9% ($8 \times 15 \text{ cm}^2$).

Another focus has been laid on edge isolation of String Ribbon cells. Results obtained for cells completely processed at Evergreen clarified that mainly the two sides containing the strings are subjected to a shunting mechanism. Different methods for edge isolation (laser grooving from front or back side, dicing) have been tested. Best improvements in fill factor have been obtained by dicing, whereas a gain in efficiency could only be achieved if the reduced cell area was taken into account.

Keywords: Ribbon Silicon - 1: Multi-Crystalline - 2: Passivation - 3

1. INTRODUCTION

The largest cost component of crystalline silicon photovoltaic modules is the cost of the silicon wafer [1]. Multicrystalline silicon wafers are cheaper to produce than monocrystalline wafers. Ribbon silicon materials are potentially even cheaper than standard cast multicrystalline wafers. This is mainly due to significantly lower costs during wafering and a better use of the silicon feedstock. Evergreen Solar's String Ribbon process [2] therefore has a high potential to significantly reduce the production costs per Wp. During crystallisation two strings provide edge stabilisation for the silicon ribbon growing between the strings directly from a silicon melt. These strings remain in the wafer throughout the whole solar cell process.

The passivation of crystal defects present in the material after crystallisation is an important step in order to improve the efficiencies of String Ribbon solar cells. Defect passivation via a hydrogen rich SiN antireflection coating is currently looked upon as the most economically favourable and effective method to reach this goal without applying additional steps during cell processing. The aim of this study was to develop a solar cell process using processing techniques which are common in an industrial environment with respect to reaching high efficiencies. In this way limitations caused either by individual processing steps currently used at Evergreen Solar or by the ribbon silicon material itself can be determined. Starting from the results of this investigation the industrial process can be further optimised if the processing steps are economically favourable.

2. CELL PROCESSING

The initial wafer size for the investigation was $8 \times 10 \text{ cm}^2$ as compared to a standard cell size of $8 \times 15 \text{ cm}^2$ normally used at Evergreen's production, and the bulk resistivity of the material was 1.5 Ohm cm . The cell processes consist of a P-diffusion, PECVD (plasma enhanced chemical vapour deposition) SiN deposition, front and back contact metallisation and a subsequent cofiring step. Wafers in different stages of processing have been exchanged between Evergreen Solar and University of Konstanz (UKN). In this way a detailed investigation and comparison of single processing steps was possible showing their influence on finished solar cell parameters. Special attention was paid to edge isolation after cell processing. Different methods like laser scribing from front or back side, sawing from front or back side or no edge isolation at all have been tested. Final cell size is 80 cm^2 in the case of no edge-isolation or laser scribing, slightly less in the case of sawing and subsequent breaking of the edge.

2.1 Processing Steps

In Fig. 1 the process sequence used at UKN is shown. The process contains a POCl_3 emitter diffusion (both sides diffused) resulting in a $40 \text{ } \Omega/\text{sq}$ emitter, a standard PECVD SiN deposition, screen printing of front and back side followed by a cofiring step for contact formation. Edge isolation was performed by sawing. During the cofiring step hydrogen from the PECVD SiN is released into the bulk of the solar cell and passivates crystal defects. Isolation of the edges was performed after an initial IV-characterisation.

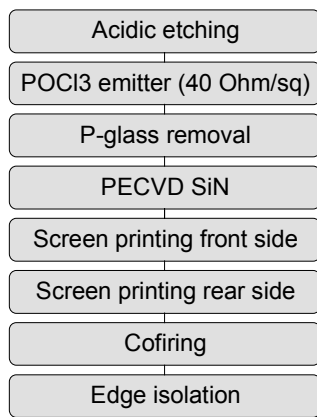


Figure 1: Process sequence for String Ribbon solar cells fabricated at UKN.

One aim of this study was to determine the potential of the String Ribbon material currently produced at Evergreen Solar concerning efficiency. The other one was to compare processing steps carried out in Evergreen's solar cell production line with those belonging to the UKN firing through the SiN process schematically shown in Fig. 1. Therefore partly processed wafers in different stages of processing have been shipped from Evergreen Solar to UKN and vice versa. Two reference batches have been processed completely at Evergreen and UKN respectively. Results from these batches are given in Fig. 2.

A gap of 1.7% absolute in efficiency could be detected between the Evergreen and UKN processes after edge isolation using a conventional wafer dicing saw and tabbing of the busbars (averaged UKN cell process parameters: 596 mV, 30.8 mA/cm², 76.8% FF, 14.1% η). The best cell of the UKN process showed an efficiency η of 14.3% (8x10 cm²) using a 40 Ω /sq emitter. Higher sheet resistivities should easily lead to efficiencies >14.5% in the near future. The width of the front grid fingers for the UKN process was approximately 200 μ m, therefore an optimisation of this screen printing step should increase the efficiency further.

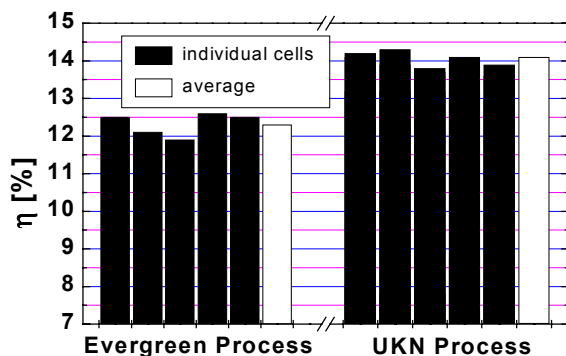


Figure 2: Comparison of cell efficiencies for two batches of solar cells after edge isolation by dicing. The cells completely processed at UKN show a 1.7% higher efficiency as compared to the cells completely processed at Evergreen Solar (14.1% as compared to 12.4% averaged over 5 cells, cell size 8x10 cm²).

By exchanging the single processing steps the influence of each step (diffusion, SiN, metallisation) on efficiency could be detected, which may help to increase the efficiency in Evergreen's production.

The interactive experiments performed between Evergreen and UKN showed no significant difference in the firing profile, an improvement of approximately 0.2% absolute in efficiency with UKN SiN deposition, and an improvement of >1% absolute in efficiency with UKN diffusion.

Process improvements on Evergreen's line that have been implemented since these experiments were performed have brought production cell efficiency averages above 12.5% without edge isolation. These improvements were primarily in the areas of Si growth, SiN deposition, metallisation procedure, and firing profile. FF averages are still low with average values <72%. A reduction of edge leakage as guided by this work should bring average efficiencies well over 13%. Improvements to the diffusion process should bring efficiencies even higher. Evergreen R&D activities in crystal growth and cell processing are currently focusing on ways to reduce edge leakage that do not involve cutting of the edges. The best String Ribbon cell processed at Evergreen to date showed an efficiency of 13.9%, $V_{oc} = 595$ mV, $J_{sc} = 32.0$ mA/cm², FF = 72.9% (8x15 cm²).

2.2 Bulk Passivation

Bulk passivation of crystal defects is achieved by depositing a hydrogen rich PECVD SiN layer as an antireflective coating with a following firing through step of the front contact releasing the hydrogen into the Si bulk. At the firing temperature hydrogen diffuses deep into the bulk volume because of the low interstitial oxygen concentration ($[O_i] < 10^{17}$ cm⁻³, [3]) passivating the defects. In Fig. 3 the external quantum efficiency (EQE) at 980 nm (penetration depth approx. 100 μ m) of a cell totally processed at UKN is shown. Most areas reveal a very good EQE signal with corresponding diffusion lengths large enough to reach sufficient efficiencies. Only relatively small areas of the cell show a low EQE signal. They can be found mainly at the upper and lower part of the cell where the strings are located and therefore crystal grains are considerably smaller. But there is also an area visible on the right where hydrogenation via the PECVD SiN was also not sufficient. This behaviour in String Ribbon material was also detected and investigated in another study [4].

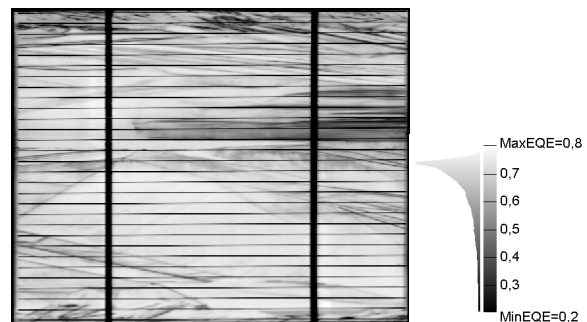


Figure 3: EQE at 980 nm of a String Ribbon solar cell (8x10 cm²) completely processed at UKN.

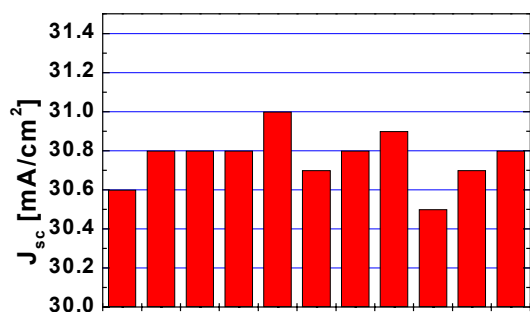


Figure 4: J_{sc} of String Ribbon cells processed completely at UKN. The narrow distribution demonstrates the homogeneous material quality on the scale of the cell size ($8 \times 10 \text{ cm}^2$).

Nevertheless, all cells processed using the complete UKN process show a very narrow distribution of short circuit current densities (J_{sc}), as can be seen from Fig. 4. This indicates that the fraction of areas which can not be sufficiently passivated by hydrogen is more or less constant within the scale of the cell size ($8 \times 10 \text{ cm}^2$). After improving the short wavelength part of the EQE by using a higher sheet resistivity, a further increase in J_{sc} could be achieved if diffusion lengths within these highly defective areas can be improved. This could be achieved by an optimisation of the crystallisation process.

3. EDGE ISOLATION

Edge isolation of String Ribbon solar cells may be a crucial step of the solar cell process; therefore emphasis was laid on testing of different methods. The most common technique used in industry is plasma etching using a coin stack of cells to prevent the plasma from etching and damaging the cell's surface. This method is not applicable in the case of String Ribbon because the wafers are not perfectly flat and this prohibits sealing of the cell surface using the next cell's rear side. But other methods like sawing or laser grooving from front or back side have been tested on String Ribbon cells originating from Evergreen's production (cell size $8 \times 15 \text{ cm}^2$).

3.1 Cells without Edge Isolation

At the beginning of the investigation a non-isolated String Ribbon solar cell was studied. Thermography [5] has been carried out at 10 Hz lock-in frequency in order to determine and locate the main shunting mechanisms. The spatial distribution of shunts within the non-isolated cell is

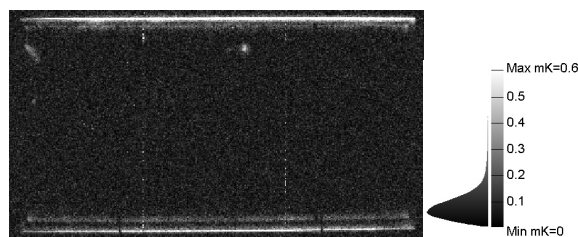


Figure 5: Thermography mapping of a String Ribbon cell ($8 \times 15 \text{ cm}^2$) without edge isolation. Shunting occurs mainly at the long sides of the cell where the strings are located.

shown in Fig. 5. Shunting occurs mainly at the long sides of the cell containing the strings. Only a weak contrast is visible within the cell area. The bright contrast inside the cell area running parallel to the outer contrast visible at the cell's edges is an artefact resulting from the difference in emissivity of silicon (outer part of the cells rear side, lower emissivity) and aluminium (inner part of the cell's rear side, higher emissivity). The two lines running vertically through the picture are artefacts too.

3.2 Methods for Edge Isolation of String Ribbon Cells

Five different methods have been tested. A very elegant method would be the cut of a laser groove at the back side near the cells edge (method A). In this way only the contacted base region would be isolated from the front side; the active area of the cell is not affected. If the laser groove is cut on the front side of the cell (method B), the active area of the cell is reduced by a fraction of the area lying in between the groove and the cell's edge. Detailed optimisation work of the pn-junction isolation properties of the laser cutting has been carried out especially for this study on standard ingot cast wafers. Edge isolation from the front side using a conventional dicing saw with subsequent breaking of the edges (method C) is the most effective way of isolation, but again the active area of the cell (in this case the cell size itself) is reduced. Method C was divided in 3 subsections, C1 (sawing of all 4 sides), C2 (sawing of the 2 short sides not containing the strings) and C3 (sawing of the 2 long string containing sides). All methods have been applied to a number of cells (varying between 6 and 11) and in the following the average values before and after edge isolation are discussed.

Table I: Edge isolation methods used in this study.

A	Laser groove at back side
B	Laser groove at front side
C1	Sawing of all 4 sides
C2	Sawing of 2 short sides (no strings)
C3	Sawing of 2 long sides (strings)

3.3 Cell Results after Edge Isolation

All cells for this investigation were fully processed at Evergreen. Cells were characterised before and after edge isolation. The average values have been used to calculate the change in cell parameters given in Table II.

Table II: Changes in IV parameters of String Ribbon cells ($8 \times 15 \text{ cm}^2$) due to edge isolation (mean values). The reduced active cell area for methods B and C was not taken into account.

Method (no. of cells)	ΔFF [% _{abs}]	ΔV_{oc} [mV]	ΔI_{sc} [mA]	$\Delta \eta$ [% _{abs}]
A (6)	-0.5	+0.8	-10.3	-0.15
B (11)	+0.2	+2.2	-26.6	-0.01
C1 (6)	+2.4	+1.2	-156.0	-0.11
C2 (10)	-0.3	-0.1	-45.3	-0.20
C3 (7)	+1.2	+0.2	-101.2	-0.16

Concerning the edge isolation effect, FF and V_{oc} have to be analysed. Lasering from the back side (A) shows almost no effect on FF and V_{oc} , although the same parameters developed for this study led to good results in another investigation using standard cast material fully processed at UKN [6]. Lasering from the front side improves V_{oc} significantly, but the effect on FF is poor. The reason for this poor improvement of FF is the damage of the space charge region resulting in an increased saturation current density J_{02} [6]. Dicing of all 4 sides from the front side (C1) leads to the highest increase in FF, whereas dicing of the short sides (C2) does not improve FF in contrast to dicing the long sides containing the strings (C3). Together with the results from section 3.1 (Fig. 5) we conclude that after processing edge isolation is already sufficient at the edges of short sides of the cells, whereas isolation at the long sides can be improved. This can be deducted qualitatively as well from Table III where the FF improvement per cm cut length is listed for the methods under investigation, although the statistics remain poor.

Table III: Gain in FF calculated as gain per cm cut length.

Method (no. of cells)	ΔFF [% _{abs}]	Distance [cm]	$\Delta FF/Distance$ [% _{abs} /cm]
A (6)	-0.5	46	-0.011
B (11)	+0.2	46	0.004
C1 (6)	+2.4	46	0.052
C2 (10)	-0.3	16	-0.018
C3 (7)	+1.2	30	0.040

Concerning economy, the power per cell has to be taken into account. As the methods revealing an improved isolation effect reduce the active area of the cell, short circuit current (I_{sc}) is reduced for these methods resulting in an overcompensation of the beneficial edge isolation effect. Therefore no gain in power could be detected for all methods under investigation (Table II).

Results look different if the reduced active area of the cells after edge isolation using methods B, C1, C2 and C3 is taken into account (Table IV). Now improvements in efficiency can be obtained for all methods providing a separation of the edges at the long sides from the front side (methods B, C1 and C3). The average efficiency could be increased up to 0.41% absolute in the case of sawing all 4 sides of the cell (C1).

Table IV: Changes in IV parameters of String Ribbon cells ($8 \times 15 \text{ cm}^2$) due to edge isolation (mean values). The reduced active cell area for methods B and C was taken into account (ΔI_{sc} set to 0).

Method (no. of cells)	ΔFF [% _{abs}]	ΔV_{oc} [mV]	ΔI_{sc} [mA]	$\Delta \eta$ [% _{abs}]
A (6)	-0.5	+0.8	-10.3	-0.15
B (11)	+0.2	+2.2	+0	+0.09
C1 (6)	+2.4	+1.2	+0	+0.41
C2 (10)	-0.3	+0.1	+0	-0.06
C3 (7)	+1.2	+0.2	+0	+0.20

4. SUMMARY

Large area solar cells have been processed from String Ribbon material supplied by Evergreen Solar using different processing steps carried out at University of Konstanz (UKN) and Evergreen. Between the processes totally carried out at Evergreen and UKN respectively, there was an efficiency gap of 1.7% absolute with the UKN process resulting in average efficiencies of 14.1%. The best cell showed an efficiency of 14.3% ($8 \times 10 \text{ cm}^2$) using an industrial type screen printing process. By a successive exchange of processing steps we could determine which of Evergreen's processing steps have the most room for improvement.

A special focus was laid on edge isolation of cells processed completely at Evergreen. Thermography revealed that mainly the edges at the long sides of the cells containing the strings are responsible for shunting mechanisms. Different methods for edge isolation (laser cutting from front and back side, sawing and subsequent breaking of the edges) have been optimised and tested. FF could be increased if the string containing sides are isolated by cutting from the front side. Improvements in efficiency could only be obtained if the reduced (active) cell area was taken into account.

5. ACKNOWLEDGEMENTS

We like to thank Martin Langenkamp and Pati Rakotoniaina from the MPI für Mikrostrukturphysik, Halle (Germany) for thermography measurements and discussion.

REFERENCES

- [1] T.M. Bruton, J.M. Woodcock, K. Roy, B. Garrard, J. Alonso, J. Nijs, A. Rauber, A. Valleria, H. Schade, E. Alsema, R. Hill, B. Dimmler, Multi-megawatt Upscaling of Silicon and Thin Film Solar Cell and Module Manufacturing (Music FM), publishable final European Community project report
- [2] W.M. Sachs, D. Ely and J. Serdy, Edge Stabilized Ribbon (ESR) Growth of Silicon For Low Cost Photovoltaics, *J. Cryst. Growth* **82** (1987), 117
- [3] T. Pernau, G. Hahn, M. Spiegel, G. Dietsche, Bulk Hydrogenation of mc Silicon Materials and Solar Cells: From Research Lab to PV-Industry, Proc. 17th EC PVSEC, Munich, 2001
- [4] P. Geiger, G. Kragler, G. Hahn, P. Fath, E. Bucher, Lifetime Enhancement in String Ribbon Silicon – A Study Based on Spatially Resolved Measurements, Proc. 17th EC PVSEC, Munich, 2001
- [5] M. Langenkamp, O. Breitenstein, Classification of shunting mechanisms in crystalline silicon solar cells, E-MRS spring meeting 2001, to be published in *Solar Energy Materials And Solar Cells*
- [6] A. Hauser, G. Hahn, M. Spiegel, H. Feist, P. Fath, E. Bucher, Comparison of Different Techniques for Edge Isolation, Proc. 17th EC PVSEC, Munich, 2001